RESEARCH

Start current and growth rate in Smith–Purcell free-electron laser with dielectric-loaded cylindrical grating

Zahra Rezaei[1] (ID) · Bizhan Farokhi[1]

Abstract

We present an analytic theory for Smith–Purcell device in which a cylindrical metal–dielectric grating was derived by an annular electron beam propagating along the grating axis. A dispersion relation is obtained for azimuthally symmetric modes. Also, the first-order and second-order growth rates of the modes which are in phase with the beam are compared. It is shown that the second-order growth rate gives a more accurate description of beam–wave interaction for beams with larger thicknesses, as well as grating slots, with smaller depths and greater lengths. The start current for BWO operation of the SP-FEL is presented too. The importance of the minimum value of start current is that above it, the SP-FEL will operate as an oscillator, even in the absence of external feedback. In this case, the group velocity of the synchronous evanescent wave is negative, while the electron beam travels in the forward direction. It is shown in this paper that the dielectric and grating parameters affect the value of start current. So, by changing these parameters, the minimum value for the start current can be obtained.

Keywords Smith–Purcell FEL · Beam–wave interaction · Cylindrical grating · Dielectric · Start current · Growth rate

Introduction

When an electron beam travels near a periodic metal surface (grating), parallel to it and perpendicular to its rulings, spontaneous radiation is emitted. This radiation, known as Smith–Purcell radiation, was first observed by Smith and Purcell in 1953 [1]. The SP radiation is a tunable electromagnetic source, which is given as follows:

$$\lambda = \frac{d}{n}\left(\frac{1}{\beta} - \cos\theta\right), \tag{1}$$

where β, θ, λ and n denote the relative velocity of the electron beam, the direction of the radiated wave with respect to this beam, the wavelength and the order of this radiation, respectively. The idea of developing a new kind of free-electron laser based on SP radiation seemed practical, after observing THz superradiant at currents above 1 in Dartmouth experiment [2]. Since then, a lot of theoretical and

experimental works have been done on the SP-FEL, as it is a compact size tunable THz source of radiation [2–6].

A device based on beam-grating can be operated as a laser if the SP radiation becomes coherent. SP-FEL has two operating modes. It works as a traveling wave amplifier if the electron beam and the synchronous evanescent wave both travel in the positive z-direction. The other operating mode is backward wave oscillator (BWO), where the group velocity is negative [7].

In consideration of the BWO type of SP-FEL, it was shown that if the beam current exceeds a certain threshold, known as start current, the radiation amplitude grows exponentially [7–12]. In recent years, some efforts have been done to reduce this start current, which results in easier production of high-power compact THz sources [6, 12–14]. In these researches, utilizing two identical rectangular gratings [6], loading dielectric in a rectangular grating [12], adding Bragg reflector to a grating [13] and applying two-beam interaction [14] for reducing the start current of BWO SP-FEL were suggested. In the SP oscillator considered by Schachter and Ron, the proposed theory was based on the interaction of an electron beam with a wave traveling along the grating. They predicted a small signal gain of SP-FEL to be proportional to a cubic root of the electron beam current. Their results agree with slow-wave devices such

✉ Zahra Rezaei
   rezaei.zahra1984@gmail.com

[1] Department of Physics, Faculty of Science, Arak University,
     P.O. Box 38156-8-8349, Arāk, Iran

as Cherenkov FEL [15]. Kim and Song solved the initial problem of the sheet beam, by using the interaction of the electrons with a traveling wave, and found that the gain is proportional to the square root of electron beam [16]. Later, Andrews and Brau explained the experiment of Urata, as bunching of the beam electrons due to the interaction of an evanescent wave with this sufficiently high current beam. Their calculations show that the gain of this radiation has cube root dependence on the beam current [17]. Besides, the growth rate of SP-FEL considered by Klochkov et al. [18] is proportional to the square root of the sheet electron beam current.

Bluem et al. [19] worked on a cylindrical grating exposed by an annular beam. They observed both superradiance and SP radiation. Also, Ashrafi et al. [20] proposed a waveguide loaded with dielectric. Then, they considered the effect of dielectric on the growth rate.

In the present work, the linear theory of an annular electron beam, propagating along a cylindrical grating, is analyzed. The structure is a mix of alternate dielectric and metal gratings. The threshold current for starting the BWO is given. For simplicity, we assume that the system is uniform in the direction parallel to the slots of the grating. The fundamental dynamical equations are presented in Sect 2. The results and discussion are given in Sect. 3. In the last part, the conclusion is considered.

Theory

A diagram of the proposed scheme is illustrated in Fig. 1. A cylindrical grating is made of alternative ideal metal and dielectric gratings, and its period, slot width, slot depth, inner radius and outer radius are denoted as $2d$, l, h, R_1 and R_2, respectively. An annular electron beam with inner radius a_1 and outer radius a_2 in a uniform static axial magnetic field B_0 is drifting with velocity along the axis of the grating and very close to it. We assumed that this magnetic field is so strong to omit the transverse perturbations of the emitted beam. Also,

for simplicity, the space charge effect is neglected, and the system is assumed to be uniform in the φ-direction.

Dispersion relation

The dispersion relation of the modes of this system is the result of considering Maxwell's equations with the continuity equation and the relativistic momentum equation for electron beam:

$$\nabla \times E = -\frac{\partial B}{\partial t}$$

$$\nabla \times B = \mu J + \frac{1}{c^2}\frac{\partial E}{\partial t}$$

$$\frac{\partial n}{\partial t} + \nabla \cdot (nv) = 0$$

$$\gamma^3 m_0 n_0 \left[\frac{\partial}{\partial t} v + v_{0z} \cdot \nabla v \right] = -e n_0 (E_z + v \times B). \tag{2}$$

In the following, we expand all quantities in terms of an unperturbed part plus a small perturbation: $n = n_0 + \delta n$, $v = v_0 + \delta v$, $J = J_0 + \delta J$, $E = \delta E$ and $B = B_0 \hat{z} + \delta B$, where n and v are the electron density and velocity, respectively. Unperturbed beam density, n_0, is uniform and time independent, δE and δB are the electric and magnetic fields, $J = -env$ is the density of current, $\gamma = (1 - v^2/c^2)^{-1/2}$ is the relativistic factor, and c is the velocity of light in free space. The perturbed density of current is given as follows:

$$\delta J = -e(n\delta v_z + \delta n v_{0z}), \tag{3}$$

which by the help of the continuity and momentum equations is defined as follows:

$$\delta J_z = \frac{i\omega\varepsilon_0}{\gamma^3}\frac{\omega_p^2}{(\omega - k_n v_0)^2}\delta E_z. \tag{4}$$

Here, $\omega_p^2 = \frac{ne^2}{m_0\varepsilon_0}$ is the beam plasma frequency.

Fig. 1 The diagram of the grating filled with dielectric. An annular electron beam drifting along the axial direction with an external magnetic field B_0 is plotted

We suppose that the TM mode propagates in this device. And by applying Floquet's theorem, the radiation fields take the general form

$$\delta f(r, t) = \sum_{n=0}^{\infty} \delta f_n(r) e^{i(k_n z - \omega t)}, \tag{5}$$

where f_n, $k_n = k_0 + 2n\pi/d$ and ω represent the Fourier coefficient, wave number in the axial direction and frequency of the nth mode, respectively.

First of all, the fields in regions of this configuration should be defined. We begin with the wave equation in the vacuum which is defined as follows:

$$\frac{1}{r}\frac{\partial}{\partial r}\left(r\frac{\partial}{\partial r}\delta E_z\right) + \left(-k_n^2 + \omega^2/c^2\right)\delta E_z = . \tag{6}$$

Region 1

This region $a_2 < r$ is the vacuum above the electron beam. So the fields here can be expressed as follows:

$$E_z(r, z) = \sum_{n=-\infty}^{+\infty} a_n K_0(\beta_n r) \exp[i(k_n z - \omega t)], \tag{7}$$

$$B_\varphi(r, z) = \sum_{n=-\infty}^{+\infty} \frac{i\omega}{c^2 \beta_n} a_n K_1(\beta_n r) \exp[i(k_n z - \omega t)]. \tag{8}$$

where $\beta_n = \sqrt{k_n^2 - \frac{\omega^2}{c^2}}$ and K is the modified Bessel function of the second kind.

Region 3

This region $R_2 < r < a_1$ is the gap between the electron beam and grating. The fields here are written as follows:

$$E_z(r, z) = \sum_{n=-\infty}^{+\infty} [c_n I_0(\beta_n r) + d_n K_0(\beta_n r)] \exp[i(k_n z - \omega t)], \tag{9}$$

$$B_\varphi(r, z) = \sum_{n=-\infty}^{+\infty} \frac{-i\omega}{c^2 \beta_n} [c_n I_1(\beta_n r) - d_n K_1(\beta_n r)] \exp[i(k_n z - \omega t)]. \tag{10}$$

Region 2

The fields in region 2, $a_1 < r < a_2$, where the electron beam exists, can be derived from this wave equation:

$$\frac{1}{r}\frac{\partial}{\partial r}\left(r\frac{\partial}{\partial r}E_z\right) + \left(-k_n^2 + \frac{\omega^2}{c^2}\right)\varepsilon^\Pi E_z = 0, \tag{11}$$

where $\varepsilon^\Pi = 1 - \frac{\omega_p^2}{\gamma^3(\omega - k_n v_0)^2}$ is the relative dielectric constant of the electron beam [21].

The solutions of this equation are evanescent waves and have the following forms:

$$E_z(r, z) = \sum_{n=-\infty}^{\infty} \frac{i}{\omega \epsilon_0 \varepsilon^\Pi} \{b_n [r \kappa_{2n} I_1(\kappa_{2n} r) + I_0(\kappa_{2n} r)] + b'_n [-r \kappa_{2n} K_1(\kappa_{2n} r) + K_0(\kappa_{2n} r)]\} \exp[i(k_n z - \omega t)], \tag{12}$$

$$B_\varphi(r, z) = \sum_{n=-\infty}^{+\infty} \mu [b_n I_0(\kappa_{2n} r) + b'_n K_0(\kappa_{2n} r)] \exp[i(k_n z - \omega t)]. \tag{13}$$

where $\kappa_{2n} = \sqrt{(k_n^2 - \frac{\omega^2}{c^2})\varepsilon^\Pi}$. I and K are the modified Bessel functions of the first and second kind, respectively.

Region 4

The wave equation in the groove, $0 < z < l$, is expressed as follows:

$$\frac{1}{r}\frac{\partial}{\partial r}\left(r\frac{\partial}{\partial r}E_z\right) + \left(-k_z^2 + \frac{\omega^2}{c^2}\right)E_z = 0. \tag{14}$$

The solutions of this equation are the cavity modes of the groove and can be expressed as follows:

$$E_z(r, z) = \sum_{m=0}^{\infty} e_m \left[J_0(\alpha_m r) - \frac{J_0(\alpha_m R_1)}{N_0(\alpha_m R_1)} N_0(\alpha_m R_1)\right] \cos\left(\frac{m\pi}{l+d}z\right), \tag{15}$$

$$B_\varphi(r, z) = \sum_{m=0}^{\infty} e_m \frac{i\omega}{c^2 \alpha_m} \left[-J_1(\alpha_m r) + \frac{J_0(\alpha_m R_1)}{N_0(\alpha_m R_1)} N_1(\alpha_m r)\right] \times \cos\left(\frac{m\pi}{l+d}z\right). \tag{16}$$

where $k_z = \frac{m\pi}{l+d}$ and $\alpha_m = \sqrt{\frac{\omega^2}{c^2} - k_z^2} > 0$. Also, J and N are the Bessel functions of the first and second kind, respectively.

Region 5

This region, $l < z < d$, is the dielectric part of the grating with relative permittivity . The fields here are expressed as follows:

$$E_z(r, z) = \sum_{m=0}^{\infty} E_m \left[J_0(\alpha'_m r) - \frac{J_0(\alpha'_m R_1)}{N_0(\alpha'_m R_1)} N_0(\alpha'_m r)\right] \times \cos\left(\frac{m\pi}{l+d}z\right), \tag{17}$$

$$B_\varphi(r, z) = \sum_{m=0}^{\infty} E_m \frac{i\omega\varepsilon_r}{c^2\alpha_m'} \left[-J_1(\alpha_m'r) + \frac{J_0(\alpha_m'R_1)}{N_0(\alpha_m'R_1)} N_1(\alpha_m'r) \right]$$
$$\times \cos\left(\frac{m\pi}{l+d}z\right). \tag{18}$$

where

$$\alpha_m' = \sqrt{\varepsilon_r \frac{\omega^2}{c^2} - k_z^2} > 0 \tag{19}$$

Region 6

The waves in this region, $d < z < 2d$, are as follows:

$$E_z(r, z) = \sum_{m=0}^{\infty} E_m'' \left[J_0(\alpha_m r) - \frac{J_0(\alpha_m R_1)}{N_0(\alpha_m R_1)} N_0(\alpha_m r) \right] \times \cos\left(\frac{m\pi}{l+d}z\right), \tag{20}$$

$$B_\varphi(r, z) = \sum_{m=0}^{\infty} E_m'' \frac{i\omega\varepsilon_r}{c^2\alpha_m} \left[-J_1(\alpha_m r) + \frac{J_0(\alpha_m R_1)}{N_0(\alpha_m R_1)} N_1(\alpha_m r) \right]$$
$$\times \cos\left(\frac{m\pi}{l+d}z\right). \tag{21}$$

As we assumed $k_0 d < 2\pi$, it is enough to keep just the lowest harmonic ($m = 0$) in the slots. The continuity of displacement vector at $r = R_2$, $z = l$ and $z = d$ results in:

$$e_m = \varepsilon_r \frac{H_{\alpha'}}{H_\alpha} E_m, \tag{22}$$

$$e_m = E_m'', \tag{23}$$
where

$$H_\alpha = \left[J_0(\alpha_0 R_2) - \frac{J_0(\alpha_0 R_1)}{N_0(\alpha_0 R_1)} N_0(\alpha_0 R_2) \right], \tag{24}$$

$$H_{\alpha'} = \left[J_0(\alpha_0' R_2) - \frac{J_0(\alpha_0' R_1)}{N_0(\alpha_0' R_1)} N_0(\alpha_0' R_2) \right]. \tag{25}$$

After applying the continuity conditions in the border of regions 1_2, 2_3 and 3_4,5,6, the dispersion relation will be as follows:

$$R(\omega, k_n, \varepsilon^\Pi) = 1, \tag{26}$$
where

$$R(\omega, k_n, \varepsilon^\Pi) = \sum_{n=-\infty}^{\infty} \frac{-2\sin\left[\frac{k_n(l+d)}{2}\right]}{k_n^2\beta_n d} \frac{H_\alpha}{\frac{2lH_{\alpha'}}{\alpha_0} + H_\alpha H_{\alpha'}(d-l)/\alpha_0' H_{\alpha'}}$$
$$\times \left\{ \left(\frac{1}{\varepsilon_r} - 1\right) \sin\left[\frac{k_n(-l+d)}{2}\right] + \sin\left[\frac{k_n(l+d)}{2}\right] \right\}$$
$$\times \frac{[I_1(\beta_n R_2)(A_1 A_6 - A_2 A_5) + K_1(\beta_n R_2)(A_3 A_6 - A_4 A_5)]}{[I_0(\beta_n R_2)(A_1 A_6 - A_2 A_5) - K_0(\beta_n R_2)(A_3 A_6 - A_4 A_5)]}. \tag{27}$$

Here, we have:

$$H_\alpha' = \left[-J_1(\alpha_0 R_2) + \frac{J_0(\alpha_0 R_1)}{N_0(\alpha_0 R_1)} N_1(\alpha_0 R_2) \right], \tag{28}$$

$$H_{\alpha'}' = \left[-J_1(\alpha_0' R_2) + \frac{J_0(\alpha_0' R_1)}{N_0(\alpha_0' R_1)} N_1(\alpha_0' R_2) \right], \tag{29}$$

$$A_1 = \frac{K_1(\beta_n a_1)}{\beta_n \varepsilon^\Pi a_1} \times [a_1 \kappa_{2n} I_1(\kappa_{2n} a_1) + I_0(\kappa_{2n} a_1)] + K_0(\beta_n a_1) I_0(\kappa_{2n} a_1), \tag{30}$$

$$A_2 = \frac{K_1(\beta_n a_1)}{\beta_n \varepsilon^\Pi a_1} \times [-a_1 \kappa_{2n} K_1(\kappa_{2n} a_1) + K_0(\kappa_{2n} a_1)]$$
$$+ K_0(\beta_n a_1) K_0(\kappa_{2n} a_1), \tag{31}$$

$$A_3 = \frac{-I_1(\beta_n a_1)}{\beta_n \varepsilon^\Pi a_1} \times [a_1 \kappa_{2n} I_1(\kappa_{2n} a_1) + I_0(\kappa_{2n} a_1)] + I_0(\beta_n a_1) I_0(\kappa_{2n} a_1), \tag{32}$$

$$A_4 = \frac{-I_1(\beta_n a_1)}{\beta_n \varepsilon^\Pi a_1} \times [-a_1 \kappa_{2n} K_1(\kappa_{2n} a_1) + K_0(\kappa_{2n} a_1)]$$
$$+ I_0(\beta_n a_1) K_0(\kappa_{2n} a_1), \tag{33}$$

$$A_5 = \frac{K_1(\beta_n a_2)}{\beta_n \varepsilon^\Pi a_2} \times [a_2 \kappa_{2n} I_1(\kappa_{2n} a_2) + I_0(\kappa_{2n} a_2)] + K_0(\beta_n a_2) I_0(\kappa_{2n} a_2), \tag{34}$$

$$A_6 = \frac{K_1(\beta_n a_2)}{\beta_n \varepsilon^\Pi a_2} \times [-a_2 \kappa_{2n} K_1(\kappa_{2n} a_2) + K_0(\kappa_{2n} a_2)]$$
$$+ K_0(\beta_n a_2) K_0(\kappa_{2n} a_2). \tag{35}$$

In the absence of beam ($a_1 = a_2$), the above dispersion relation becomes:

$$R_0(\omega, k)$$
$$= \sum_{n=-\infty}^{\infty} \frac{2\sin[\frac{k_n(l+d)}{2}]}{k_n^2\beta_n d} \times \frac{K_1(\beta_n R_2)}{K_0(\beta_n R_2)} \times \frac{H_\alpha}{\frac{2lH_{\alpha'}}{\alpha_0} + H_\alpha H_{\alpha'}(d-l)/\alpha_0' H_{\alpha'}}$$
$$\times \left\{ \left(\frac{1}{\varepsilon_r} - 1\right) \sin\left[\frac{k_n(-l+d)}{2}\right] + \sin\left[\frac{k_n(l+d)}{2}\right] \right\} = 1. \tag{36}$$

Growth rate and start current

So far, the dispersion relation of the modes in this configuration has been derived. In the synchronized point, where the electron beam can interact with one of the system modes (ω_r, k_r), the growth of this mode can occur. To facilitate the calculations of the growth rate, Taylor expansion of the dispersion relation, Eq. (26), can be used, keeping the terms up to the second-order and near the solution below:

$$R(\omega_r, k_r) = 1. \tag{37}$$

So, Eq. (26) will become:

$$
\begin{aligned}
\sum_{p=1}^{2} & \frac{(\delta\omega)^p R_\omega^{(p)}}{p!} + \frac{(\delta k)^p R_k^{(p)}}{p!} + \frac{(\varepsilon^\Pi - 1)^p R_{\varepsilon^\Pi}^{(p)}}{p!} \\
& + \delta\omega(\varepsilon^\Pi - 1) \frac{\partial^2 R(\omega, k_n, \varepsilon^\Pi)}{\partial\omega\partial\varepsilon^\Pi}\Big|_{(\omega_r,k_r,1)} \\
& + \delta\omega\delta k \frac{\partial^2 R(\omega, k_n, \varepsilon^\Pi)}{\partial\omega\delta k}\Big|_{(\omega_r,k_r,1)} \\
& + \delta k(\varepsilon^\Pi - 1) \frac{\partial^2 R(\omega, k_n, \varepsilon^\Pi)}{\partial k\partial\varepsilon^\Pi}\Big|_{(\omega_r,k_r,1)} = 0.
\end{aligned}
\tag{38}
$$

Here, we have:

$$
\begin{aligned}
& \delta\omega = \omega - \omega_r, \quad \delta k = k - k_r \\
& R_{\varepsilon^\Pi}^{(p)} = \frac{\partial^p R(\omega, k_n, \varepsilon^\Pi)}{\partial(\varepsilon^\Pi)^p}\Big|_{(\omega_r,k_r,1)}, \\
& R_k^{(p)} = \frac{\partial^p R(\omega, k_n, \varepsilon^\Pi)}{\partial k^p}\Big|_{(\omega_r,k_r,1)} = \frac{\partial^p R_0(\omega, k_n)}{\partial k^p}\Big|_{(\omega_r,k_r)}, \\
& R_\omega^{(p)} = \frac{\partial^p R(\omega, k_n, \varepsilon^\Pi)}{\partial\omega^p}\Big|_{(\omega_r,k_r,1)} = \frac{\partial^p R_0(\omega, k_n)}{\partial\omega^p}\Big|_{(\omega_r,k_r)}.
\end{aligned}
\tag{39}
$$

In Eq. (38), it is enough to keep only the zeroth-order space harmonic ($n=0$). That is reasonable, because the electron beam can be synchronized only with this harmonic [22]. So, we expand $(\varepsilon^\Pi - 1)$ about (ω_r, k_r) to take the following form:

$$(\varepsilon^\Pi - 1) = -\frac{\omega_p^2}{\gamma^3 (\delta\omega - v_0\delta k)^2}. \tag{40}$$

Substituting this back in Eq. (38), a sixth-order equation is derived. This equation can be numerically solved to obtain $\delta\omega$. $\mathrm{Im}(\delta\omega)$ and $\mathrm{Re}(\delta\omega)$ would be the growth rate and frequency shifting of the unstable mode, respectively. Besides, the maximum growth occurs if we assume $\delta k = 0$ and only $\delta\omega$ is complex.

To estimate the start current, we take into account just the first-order terms in the dispersion relation in Eq. (38) as follows:

$$\delta\omega R_\omega^{(1)} + \delta k R_k^{(1)} + (\varepsilon^\Pi - 1) R_{\varepsilon^\Pi}^{(1)} = 0. \tag{41}$$

Also, $R_\omega^{(1)}$ and $R_k^{(1)}$ can be related to each other, if we differentiate the dispersion curve of Eq. (37):

$$\frac{dR}{dk} = R_\omega^{(1)} v_g + R_k^{(1)} = 0, \tag{42}$$

where $v_g = \frac{d\omega}{dk}$ and we consider $v_g < 0$ for the oscillator operating. After substituting Eqs. (40) and (42) back in Eq. (41), the dispersion Eq. (41) will be simplified as follows:

$$(\delta\omega - v_g\delta k)(\delta\omega - v_0\delta k)^2 = \Delta, \tag{43}$$

where

$$\Delta = \frac{\omega_p^2 R_{\varepsilon^\Pi}^{(1)}}{\gamma^3 R_\omega^{(1)}}. \tag{44}$$

For convenience, we rewrite Eq. (43) in dimensionless form [7] as:

$$\delta_j^2(\delta_j - \tau) - 1 = 0, \tag{45}$$

where

$$\delta_j = \left|\frac{v_0^2 v_g}{\Delta}\right|^{1/3} \left(\frac{\delta\omega}{v_0} - \delta k_j\right), \tag{46}$$

$$\tau = \left|\frac{v_0^2 v_g}{\Delta}\right|^{1/3} \left(\frac{1}{v_0} - \frac{1}{v_g}\right)\delta\omega. \tag{47}$$

The dispersion relation (43) is a cubic equation whose roots correspond to three modes. In this step, we represent the electric field of the beam as a sum of the fields of these three modes. Then, the boundary conditions must be applied to these modes to obtain the threshold current. From Eq. (12), the field of the th mode is represented as follows:

$$
\begin{aligned}
E_{z,j} = \sum_{n=-\infty}^{\infty} \frac{i}{\omega\varepsilon_0\varepsilon^\Pi} & \Big\{ b_n^j \Big[r\kappa_{2n}^j I_1(\kappa_{2n}^j r) + I_0(\kappa_{2n}^j r) \Big] \\
& + b_n'^j \Big[-r\kappa_{2n}^j K_1(\kappa_{2n}^j r) + K_0(\kappa_{2n}^j r) \Big] \Big\} \\
& \exp[i(k_0 z - \omega_0 t)] \exp[i(\delta k_j z - \delta\omega_j t)].
\end{aligned}
\tag{48}
$$

We can take the coefficients b_n^j, $b_n'^j$ and κ_{2n}^j to be identical, in the lowest order. So, the field at any time takes the following form:

$$E_z = \sum_{j=1}^{3} B_j E_j = E_0 \sum_{j=1}^{3} B_j \exp[i(\delta k_j z - \delta\omega_j t)]. \tag{49}$$

Here, the coefficient B_j is a constant and the coefficient E_0 is defined as follows:

$$E_0 = \sum_{n=-\infty}^{\infty} \frac{i}{\omega \varepsilon_0 \varepsilon^{\Pi}} \left\{ b_n \left[r\kappa_{2n} I_1(\kappa_{2n} r) + I_0(\kappa_{2n} r) \right] \right. \tag{50}$$
$$\left. + b_n' \left[-r\kappa_{2n} K_1(\kappa_{2n} r) + K_0(\kappa_{2n} r) \right] \right\} \exp[i(k_0 z - \omega_0 t)].$$

The first and second boundary conditions applied on this field arise from the fact that the density and velocity of the beam are not disturbed at the left end of the grating, where the beam enters. So, the polarization of the beam and the convective derivative of this polarization are zero:

$$P_z = -\varepsilon_0 \frac{\omega_p^2}{\gamma^3(\delta\omega - v0\delta k)^2} E_z$$
$$= -\varepsilon_0 \frac{\omega_p^2}{\gamma^3} E_0 \sum_{j=1}^{3} B_j \frac{\exp[i(\delta k_j z - \delta\omega_j t)]}{\left(\delta\omega_j - v_0\delta k_j\right)^2} = 0, \tag{51}$$

$$\frac{\mathrm{d}p_z}{\mathrm{d}t} = \left(\frac{\partial}{\partial t} + v_0 \frac{\partial}{\partial z} \right) p_z$$
$$= i\varepsilon_0 \frac{\omega_p^2}{\gamma^3} E_0 \sum_{j=1}^{3} B_j \frac{\exp[i(\delta k_j z - \delta\omega_j t)]}{\left(\delta\omega_j - v_0\delta k_j\right)} = 0. \tag{52}$$

Here, the polarization is written with the aid of Eq. (40). The third boundary condition is that the input field at the right end of the grating of length Z is zero:

$$E_z = E_0 \sum_{j=1}^{3} B_j \exp[i(\delta k_j Z - \delta\omega_j t)] = 0. \tag{53}$$

It should be noted that the oscillator mode of SP-FEL is possible only if all the three modes have the same frequency shift $\delta\omega_j = \delta\omega$. So, the boundary conditions can be written in the dimensionless form as follows:

$$\sum_{j=1}^{3} \frac{B_j}{\delta_j^2} = 0,$$
$$\sum_{j=1}^{3} \frac{B_j}{\delta_j} = 0, \tag{54}$$
$$\sum_{j=1}^{3} B_j \exp(-i\delta_j \xi) = 0.$$

Here,

$$\xi = \left| \frac{\Delta}{v_0^2 v_g} \right|^{1/3} Z. \tag{55}$$

For nontrivial solution to exist, the coefficients should have zero determinant; therefore,

$$\det \begin{bmatrix} 1/\delta_1^2 & 1/\delta_2^2 & 1/\delta_3^2 \\ 1/\delta_1 & 1/\delta_2 & 1/\delta_3 \\ \exp(-i\delta_1\xi) & \exp(-i\delta_2\xi) & \exp(-i\delta_3\xi) \end{bmatrix} = 0. \tag{56}$$

Equations (45) and (56) are solved numerically, and it has been shown that if the minimum value of $\xi(\xi_0)$ is 1.97, $\mathrm{Im}(\tau)$ will become nonnegative [23]. It is clear from Eq. (47) that once $\mathrm{Im}(\tau) > 0$, the imaginary part of $\delta\omega$ becomes greater than zero, and the growth of the unstable mode starts.

Finally, the threshold condition for a growing oscillation can be written as follows:

$$\xi - \xi_0 > 0. \tag{57}$$

The start current can be derived by rewriting Eq. (57) as follows:

$$\left| \frac{e}{m\varepsilon_0} \frac{I}{A} \frac{R_{\varepsilon^{\Pi}}^{(1)}}{\gamma^3 R_\omega^{(1)}} \frac{1}{v_0^3 v_g} \right|^{1/3} - \xi_0 > 0. \tag{58}$$

Results and discussion

To study the dispersion characteristics of the grating, the dispersion curves in the absence of beam are considered by solving Eq. (36) numerically. The parameters of our configuration are listed in Table 1. The dependence of the propagating modes on the structure parameters is shown in Fig. 2. In Fig. 2a, the effect of ε_r on the dispersion curves is depicted. It is clear that as the dielectric relative permittivity is increased, the curves become more like a flat shape and the intersection point of the beam and these modes decreases.

The dispersion curves for various slots depths are depicted in Fig. 2b. As the slot depth increases, the dispersion curves become lowered, and the frequencies of the beam–wave interaction go down. On the other hand, decreasing the width of the dielectric has the same effect on the

Table 1 Parameters of the system

Grating length	$Z = 6400~\mu m$
Grating period	$2d = 320~\mu m$
Groove width	$l = 80~\mu m$
Inner radius of groove	$R_1 = 240~\mu m$
Groove depth	$h = 100~\mu m$
Inner radius of e-beam	$a_1 = 340~\mu m$
Outer radius of e-beam	$a_2 = 400~\mu m$
Electron relative velocity	$\beta = .45$
Relative dielectric permittivity	$\varepsilon_r = 3.0$
Normalized beam plasma frequency	$\omega_p d/c = 1$
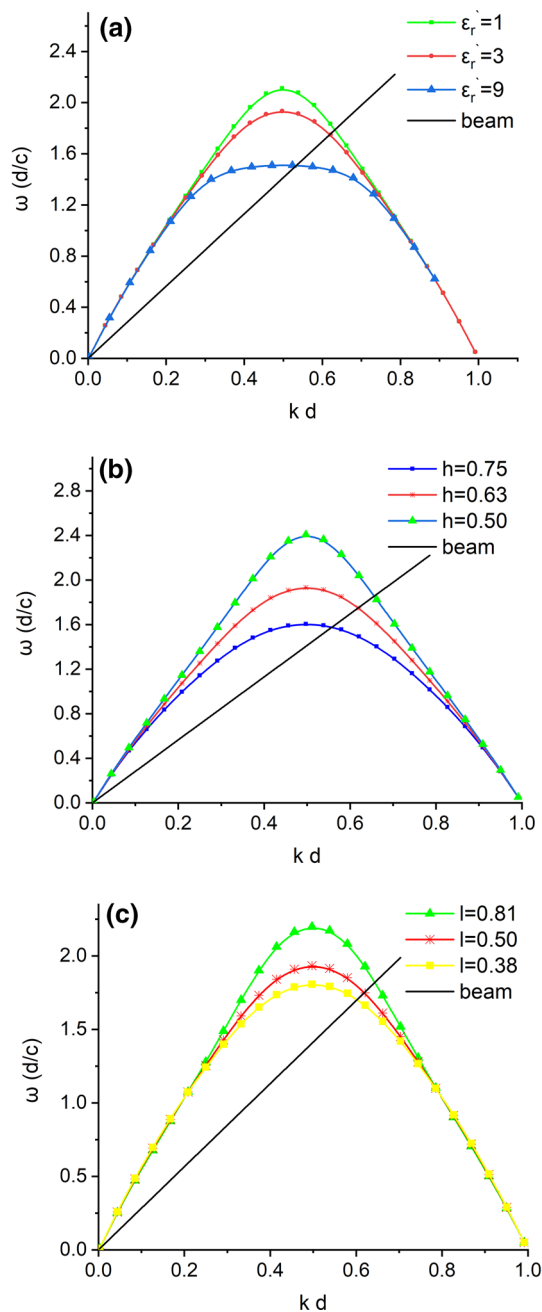
Fig. 2 Dispersion curves of cylindrical grating in the absence of beam related to the **a** relative dielectric permittivity ε_r, **b** height of the grating, **c** slot lengths. The beam line with $\beta = .45$ is plotted for reference too. The other parameters are listed in Table 1

dispersion curves, as it is clear in Fig. 2c. From this figure, we understand that lower frequencies of the interaction points are the result of decreasing the width of the dielectric.

Comparisons between the first-order and second-order growth rates, for the case $\delta k = 0$, are done by solving Eqs. (43) and (38), respectively. The results are depicted in Fig. 3 for different parameters of the system. Both the growth rate curves have similar behavior in each figure.

Figure 3a shows that the dielectric in this configuration decreases the amount of the growth rate. However, the discrepancy between the first-order and second-order growth rate is not too much, and the first-order growth rate can describe the interaction accurately. Figure 3b shows that the smaller the slot width is, the higher the growth rate will be. This is reasonable because by increasing the width, the resonance frequency increases too. So, the growth of such a high frequency is more difficult. Besides, as the width of slots extends, the discrepancy between the first-order and second-order growth rates gets larger. So, in this condition, the second-order growth rate is more precise to describe the interaction. The dependence of the growth rate on the height of slots is plotted in Fig. 3c. It is clear from the curves that slots with greater heights—in which the resonance frequency is smaller—enhance the growth rate. Moreover, the two growth rate curves approach each other gradually, as the height rises. So, using the first-order growth rate is acceptable just for higher depths. As it is indicated in Fig. 3d, the growth rate depends on the relative velocity of the beam. For small values of β, where the resonance frequency is very low, the growth rate is insignificant. Increasing β enhances the growth rate. So, the maximum growth rate happens when $\beta = 0.2$. However, when the relative beam velocity increases, as the resonance frequency rises too, the growth rate reduces. Also, the two curves of growth rates almost match each other. The effect of beam thickness on the growth rate is shown in Fig. 3e. At lower thicknesses, the growth rate is small, as the interaction of the beam with the resonant mode is not very much. However, increasing the beam thickness results in more interactions and the growth rate enhances until it reaches the saturation value. As we can see, the discrepancy between the two curves cannot be ignored when the beam thickness is not small. So, the second-order growth rate gives more accurate description of this system. In the next step, the condition for starting the SP oscillation is considered by solving Eq. (58). The effect of the relative dielectric permittivity on the start current is shown in Fig. 4a. Increasing ε_r leads to higher values for the threshold current. However, it falls for ε_r larger than about 9. In Fig. 4b, c, it is depicted that the threshold current for this oscillation is depended on the length of the grating. As the number of the grating periods increases, the electron beam can be modulated in longer distances. So, the threshold current for bunching the beam decreases significantly. The dependence of the start current on the slot depth and width is clear in Fig. 4b, c, respectively. As it is clear, the shorter the slot parameters are, the smaller the start current will become.
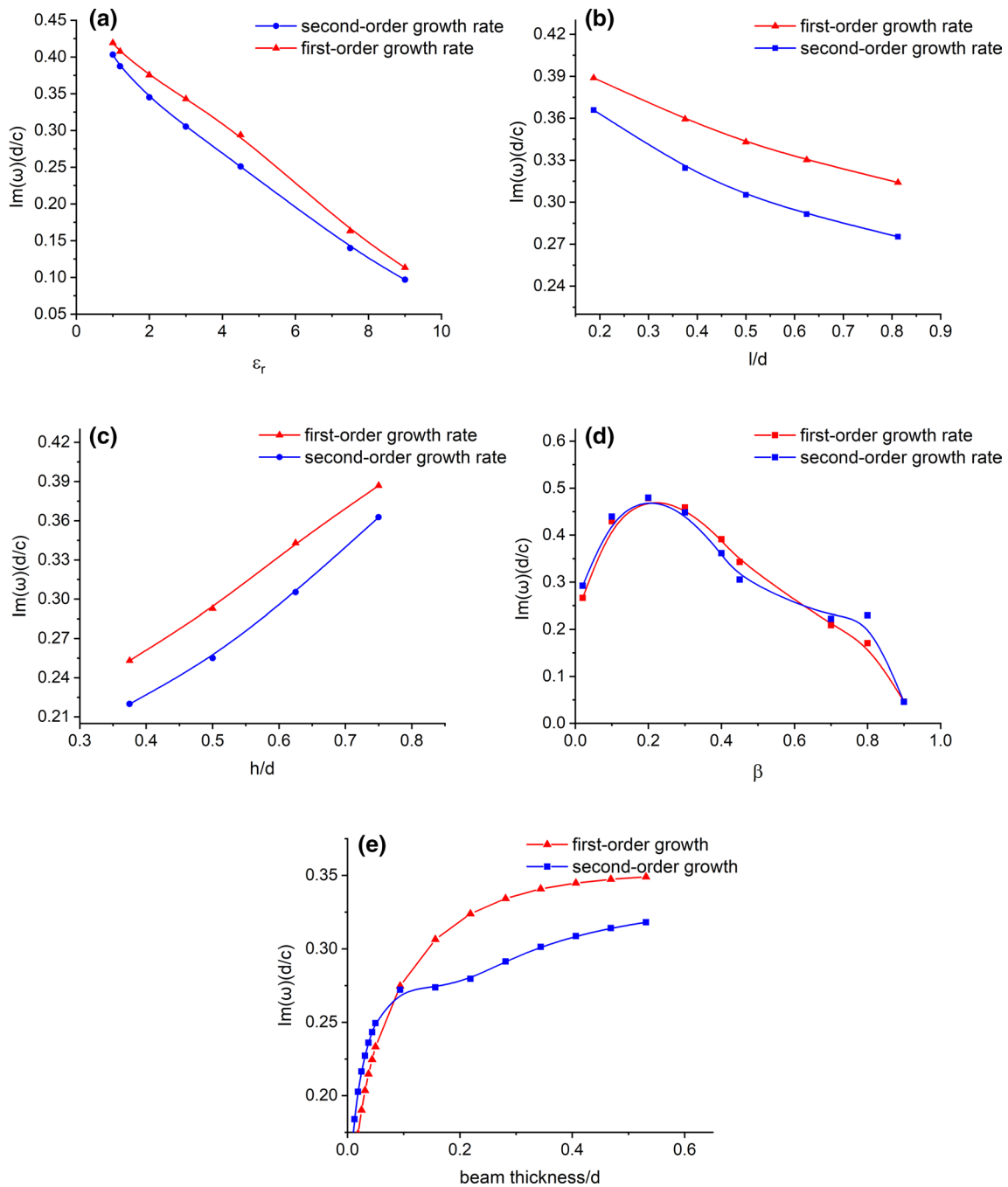
Fig. 3 The dependence of first-order and second-order growth rates on the: **a** relative dielectric permittivity ε_r, **b** length of the slots, **c** depth of the slots, **d** relative velocity of the electron beam, **e** thickness of the electron beam. The other parameters of the grating are listed in Table 1

Conclusion

In this paper, we have presented a theory of Smith–Purcell radiation from a metallic–dielectric cylindrical grating. In this configuration, the effect of grating parameters on the dispersion curves, growth rate and start current is considered. Loading dielectric and making slots with smaller lengths and higher depths lead to flatter dispersion curves and reduce the operating frequency of beam–wave interaction. Consideration of the first-order and second-order growth rates at resonance points reveals that increasing the depth and decreasing the length of the
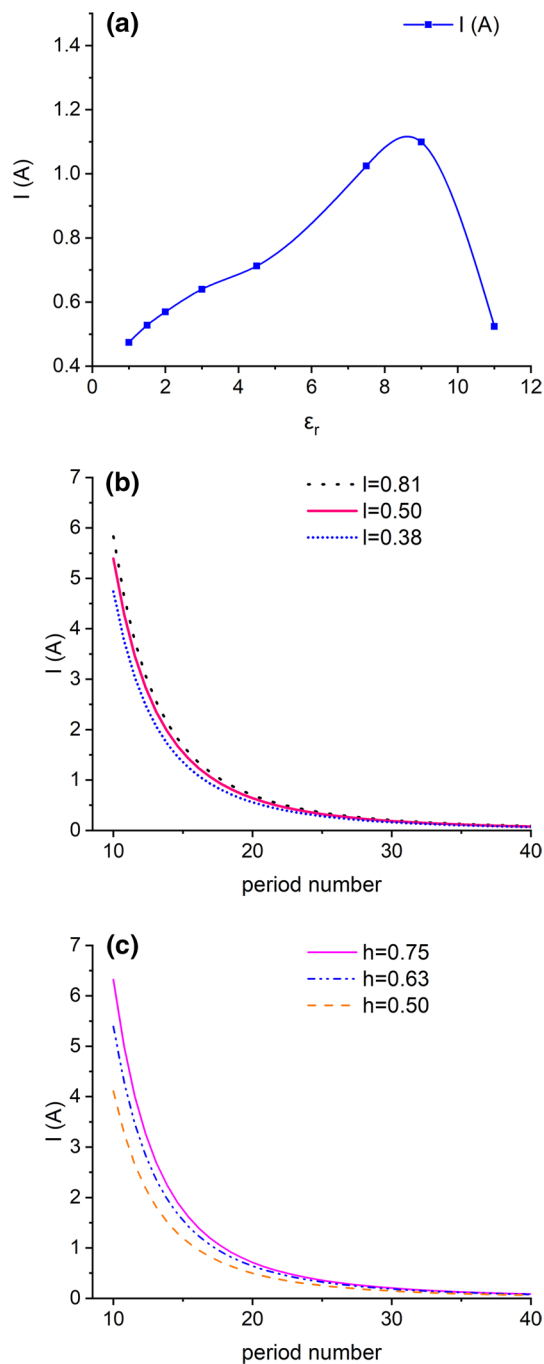
Fig. 4 The dependence of the start current on the: **a** relative dielectric permittivity ε_r, **b** total length of the grating and length of the slots, **c** total length of the grating and depth of the slots. The other parameters are listed in Table 1

slots, decreasing ε_r and also expanding the beam thickness give rise to higher values of normalized growth rate. Also, increasing the relative velocity of the beam enhances the growth first, and then, it starts to fall depending on the frequency at the operating point. Comparison between two growth curves reveals that the second-order growth

rate is more accurate especially when larger values for the slot length and beam thickness, as well as smaller ones for the slot depth, are taken. In addition, the start current required for BWO operation of SP-FEL is derived by using the boundary conditions and the dispersion relation. It is shown that increasing the relative dielectric permittivity increases the start current at first. However, the start current falls when ε_r is larger than about 9. Moreover, increasing the grating length, as well as decreasing the slot length and depth, reduces the threshold current. These results can be employed to optimize the FELs based on Smith–Purcell radiation.

References

1. Smith, S.J., Purcell, E.M.: Visible light from localized surface charges moving across a grating. Phys. Rev. **92**(4), 1069 (1953). https://doi.org/10.1103/PhysRev.92.1069
2. Urata, J., Goldstein, M., Kimmitt, M.F., Naumov, A., Platt, C., Walsh, J.E.: Superradiant Smith–Purcell emission. Phys. Rev. Lett. **80**(3), 516 (1998). https://doi.org/10.1103/physrevlett.80.516
3. Bakhtyari, A., Walsh, J.E., Brownell, J.H.: Amplified-spontaneous-emission power oscillation in a beam–wave interaction. Phys. Rev. E: Stat. Nonlin. Soft Matter Phys. **65**(6 Pt 2), 066503 (2002). https://doi.org/10.1103/PhysRevE.65.066503
4. Klochkov, D.N., Oganesyan, K.B., Ayryan, E.A., Izmailian, N.S.: Generation of induced Smith–Purcell radiation: free-electron laser in open system. J. Mod. Opt. **63**(7), 653–659 (2015). https://doi.org/10.1080/09500340.2015.1088969
5. Li, D., Wang, Y., Nakajima, M., Tani, M., Hashida, M., Asakawa, M.R., Wei, Y., Miyamoto, S.: Coherent radiation at the fundamental frequency by a Smith–Purcell free-electron laser with dielectric substrate. Appl. Phys. Lett. **110**(15), 151108 (2017). https://doi.org/10.1063/1.4980046
6. Liu, W., Lu, Y., Wang, L., Jia, Q.: A compact terahertz free-electron laser with two gratings driven by two electron-beams. Phys. Plasmas **24**(2), 023103 (2017). https://doi.org/10.1063/1.4976122
7. Andrews, H.L., Boulware, C.H., Brau, C.A., Jarvis, J.D.: Dispersion and attenuation in a Smith–Purcell free electron laser. Phys. Rev. Spec. Top. Accel. Beams **8**(5), 050703 (2005). https://doi.org/10.1103/physrevstab.8.050703
8. Kumar, V., Kim, K.J.: Analysis of Smith-Purcell free-electron lasers. Phys. Rev. E: Stat. Nonlin. Soft Matter Phys. **73**(2 Pt 2), 026501 (2006). https://doi.org/10.1103/PhysRevE.73.026501
9. Andrews, H.L., Boulware, C.H., Brau, C.A., Donohue, J.T., Gardelle, J., Jarvis, J.D.: Effect of reflections and losses in Smith–Purcell free-electron lasers. New J. Phys. **8**(11), 289 (2006). https://doi.org/10.1088/1367-2630/8/11/289

10. Kim, K.-J., Kumar, V.: Electron beam requirements for a three-dimensional Smith–Purcell backward-wave oscillator for intense terahertz. Radiation **10**(8), 080702 (2007). https://doi.org/10.1103/physrevstab.10.080702

11. Jarvis, J.D., Andrews, H.L., Brau, C.A.: Small-signal theory of a grating-based free-electron laser in three dimensions. Phys. Rev. Spec. Top. Accel. Beams **13**(2), 020701 (2010). https://doi.org/10.1103/physrevstab.13.020701

12. Liu, W., Cao, M., Wang, Y., Li, K.: Start current of dielectric-loaded grating in Smith–Purcell radiation. Phys. Plasmas **23**(3), 033104 (2016). https://doi.org/10.1063/1.4942945

13. Li, D., Imasaki, K., Gao, X., Yang, Z., Park, G.-S.: Reduce the start current of Smith–Purcell backward wave oscillator by side-wall grating. Appl. Phys. Lett. **91**(22), 221506 (2007). https://doi.org/10.1063/1.2819075

14. Liu, W., Yang, Z., Liang, Z., Li, D., Imasaki, K., Shi, Z., Lan, F., Park, G.-S.: Enhancement of terahertz Smith–Purcell radiation by two electron beams. Nucl. Instrum. Methods Phys. Res. Sect. A **580**(3), 1552–1558 (2007). https://doi.org/10.1016/j.nima.2007.07.133

15. Schachter, L., Ron, A.: Smith–Purcell free-electron laser. Phys. Rev. A Gen. Phys. **40**(2), 876–896 (1989). https://doi.org/10.1103/physreva.40.876

16. Kim, K.-J., Song, S.-B.: Self-amplified spontaneous emission in Smith–Purcell free-electron lasers. Nucl. Instrum. Methods Phys. Res. Sect. A **475**(1–3), 158–163 (2001). https://doi.org/10.1016/s0168-9002(01)01576-5

17. Andrews, H.L., Brau, C.A.: Gain of a Smith–Purcell free-electron laser. Phys. Rev. Spec. Top. Accel. Beams **7**(7), 070701 (2004). https://doi.org/10.1103/physrevstab.7.070701

18. Klochkov, D.N., Artemyev, A.I., Oganesyan, K.B., Rostovtsev, Y.V., Scully, M.O., Hu, C.-K.: The dispersion equation of the induced Smith-Purcell instability. Phys. Scr. (2010). https://doi.org/10.1088/0031-8949/2010/t140/014049

19. Bluem, H.P., Jackson, R.H., Jarvis, J.D., Todd, A.M.M., Gardelle, J., Modin, P., Donohue, J.T.: First lasing from a high-power cylindrical grating Smith–Purcell device. IEEE Trans. Plasma Sci. **43**(9), 3176–3184 (2015). https://doi.org/10.1109/tps.2015.2464074

20. Ashrafi, A., Hasanbeigi, A., Mehdian, H.: Dispersion and growth characteristics in a circular waveguide loaded with alternate metal and dielectric discs. AIP Adv. **8**(1), 015322 (2018). https://doi.org/10.1063/1.5017747

21. Cao, M., Liu, W., Wang, Y., Li, K.: Dispersion characteristics of three-dimensional dielectric-loaded grating for terahertz Smith–Purcell radiation. Phys. Plasmas **21**(2), 023116 (2014). https://doi.org/10.1063/1.4866157

22. Li, D., Hangyo, M., Tsunawaki, Y., Yang, Z., Wei, Y., Miyamoto, S., Asakawa, M.R., Imasaki, K.: Growth rate and start current in Smith–Purcell free-electron lasers. Appl. Phys. Lett. **100**(19), 191101 (2012). https://doi.org/10.1063/1.4711803

23. Swegle, J.A.: Starting conditions for relativistic backward wave oscillators at low currents. Phys. Fluids **30**(4), 1201 (1987). https://doi.org/10.1063/1.866269